

# **PARTICLE FILTERING BASED PROGNOSIS OF FATIGUE DELAMINATION GROWTH IN COMPOSITES USING NDE METHODS**

*Portia Banerjee<sup>1</sup>, Rajendra Prasath Palanisamy<sup>2</sup>, Ciaron Hamilton<sup>3</sup>, Lalita Udpa<sup>1</sup>, Mahmood Haq<sup>2,4</sup> and Yiming Deng<sup>1</sup>*

<sup>1</sup> *Department of Electrical and Computer Engineering, Michigan State University, East Lansing, MI, USA.*

<sup>2</sup> *Department of Civil and Environmental Engineering, Michigan State University, East Lansing, MI, USA.*

<sup>3</sup> *Department of Computer Science and Engineering, Michigan State University, East Lansing, MI, USA.*

<sup>4</sup> *Composite Vehicle Research Center, Lansing, MI, USA.*

## **Abstract**

With increasing use of fiber reinforced polymer (FRP) composites in several industries such as aviation, automotive and construction, effective diagnosis and prognosis of composites have become an extremely critical task in recent years. Despite outstanding qualities of light-weight, high specific stiffness and strength, composites are often vulnerable to damages caused due to fatigue or external impacts which compromise their performance and hence propel the need of periodic inspection by robust non-destructive evaluation (NDE) techniques. Further, accurate health prognosis is critical for condition-based maintenance (CBM) and for reducing life-cycle costs by taking full advantage of remaining-useful-life (RUL) of equipment. In this paper delamination growth caused by fatigue loading in Mode I GFRP sample is periodically inspected by optical transmission scanning (OTS) and guided waves (GW), which are excited and sensed by miniature surface-mounted piezoelectric sensors (PZT). An integrated prognostics framework for estimation of damage propagation based on Bayesian updating is proposed, which utilizes exponential model and CBM data obtained from NDE techniques. Results effectively compare and demonstrate the prognostic capabilities of the two NDE methods on inspection of GFRP composites.

## **Introduction**

In last few decades, composite materials have gained immense popularity and replaced metals or alloys in several industries namely aviation, automotive, space and construction owing to their salient properties of light-weight, high specific stiffness and strength. Laminated fiber-reinforced composite materials are also known for their good environmental resistance and fatigue resistance. However, such composite structures are often vulnerable to flaws during fabrication and service such as impacts damages or disbonds in adhesive joints, which may be hidden in internal layers and barely visible on outer surfaces. Complex damage mechanisms demand the use of nondestructive evaluation (NDE) techniques such as vibration, acoustic emission, X-ray imaging etc. for inspection of composite materials [1-4]. Information about present damage state obtained from NDE of composites further facilitates prediction of future health status of structures and allows condition-based-maintenance of components in industries. Accurate health prognostics is critical for reducing overall life-cycle costs by taking full advantage of the remaining useful life (RUL) of a component.

Industrial components made of composite materials are often subjected to a wide spectrum of loading during their in-service use resulting into fatigue-induced delamination at the joints, which pose serious threat to their remaining usability and reliability. Although several analytical and experimental investigations [5-6] have been conducted on the initiation and evolution of fatigue damages in composite materials, prognosis of fatigue-induced damage in composites remains a challenging task due to highly uncertain nature of fatigue progression in the matrix laminates [7]. Fatigue crack or delamination in composites depends on the manufacturing process, material, and presence of impurities or inclusions in resin or other complex micro-level phenomenon, which are difficult to incorporate into physics based models. Hence, stochastic approach is the logical choice for prognosis of fatigue damage growth in composite joints.

In this paper, the prognostic capability of two NDE approaches is assessed on GFRP composite. Firstly, optical transmission scanning (OTS) is used to diagnose damage introduced in a mode 1 GFRP sample by cyclic loading. OTS is a novel optical method for quantitative NDE of GFRP structures proposed by Khomeenko et al. [8]. Apart from being non-contact, rapid and cost-efficient, it provides high-resolution scans of GFRP samples. In addition to OTS, Guided Wave (GW) based technique is used on the same sample to measure delamination growth. This technique involves piezoelectric actuators and sensors in a pitch-catch configuration [9]. The paper presents two crucial contributions to research in NDE of composite materials utilizing experimental data from OTS and GW of GFRP samples. Firstly, an optimized yet simple damage propagation model is presented describing growth of delamination area in the sample. Secondly, an integrated prognosis method is implemented to estimate damage area growth in GFRP wherein data from OTS and GW are used for estimation of the future damage area under the framework of particle-filtering. With growing demand of GFRP in industries, prognostic studies on such materials have become imperative and are therefore addressed in this study.

## **Materials and Methods**

### **Fatigue testing**

Fatigue is a progressive, localized, permanent structural change that occurs in materials subjected to fluctuating stresses and strains that may result in cracks or fractures after a sufficient number of fluctuations. Damage due to fatigue arises at axial loading much lower than the critical load limit. Although progressing at a lower rate, fatigue can induce local matrix cracking leading to global damages in adhesive joints or matrix laminates, which significantly compromises structure's health and can be catastrophic. Owing to its industrial importance, fatigue mechanisms have been studied extensively with regards to composite materials [10-12]. Usually fatigue results in loss of stiffness or strength of the material characterizing joints in FRP structures. In this work the delamination area in a mode 1 GFRP sample is considered as the damage variable to investigate effect of fatigue in GFRP resin, given that it can be monitored using NDE methods.

### **Delamination detection using Optical Transmission Scanning(OTS)**

One of the NDE techniques used in this study to diagnose the extent of delamination in the GFRP sample subjected to fatigue testing is the OTS system [13]. Figure 1 shows the image of the OTS setup. It comprises a translation stage, a laser source that illuminates the GFRP samples, and a downstream photodetector placed underneath the sample. The photodetector records the power transmitted through the sample after it is illuminated by the laser source.

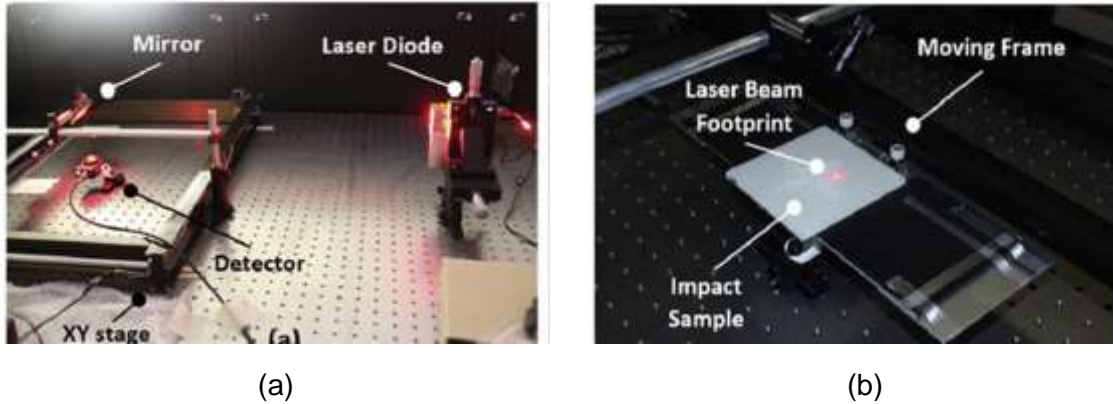


Figure 1. (a) Experimental set-up of Optical Transmission Scan system (b) Sample under OTS.

A detailed description of the OTS operating principle in a GFRP sample at a given scan position is provided in [8,13]. Since the photodetector records the power transmitted through the sample, output from OTS systems primarily depends on the transmission properties of the sample being tested. Presence of delamination (air gap) inside the sample creates a mismatch of refractive index between the two materials resulting in partial reflection of induced light. Power loss alters transmitted radiation received by the photodetector, which indicates the location and extent of delamination inside the sample. An image of a GFRP sample with surface delamination inspected by OTS imaging system is depicted in Figure 2. As opposed to traditional ultrasonic imaging techniques, OTS is a non-contact method with rapid scanning time. Further, Khomenko et al. successfully demonstrated OTS as a valid technique to detect delamination in GFRP induced by repeated low-velocity impacts and validated scanned results by observing damage in a cross-section of the impacted samples after being cut by diamond-saw. Similar to crack length in fatigue-crack-growth (FCG) prediction, delamination area serve as a suitable health indicator of a mode 1 GFRP sample subjected to fatigue.

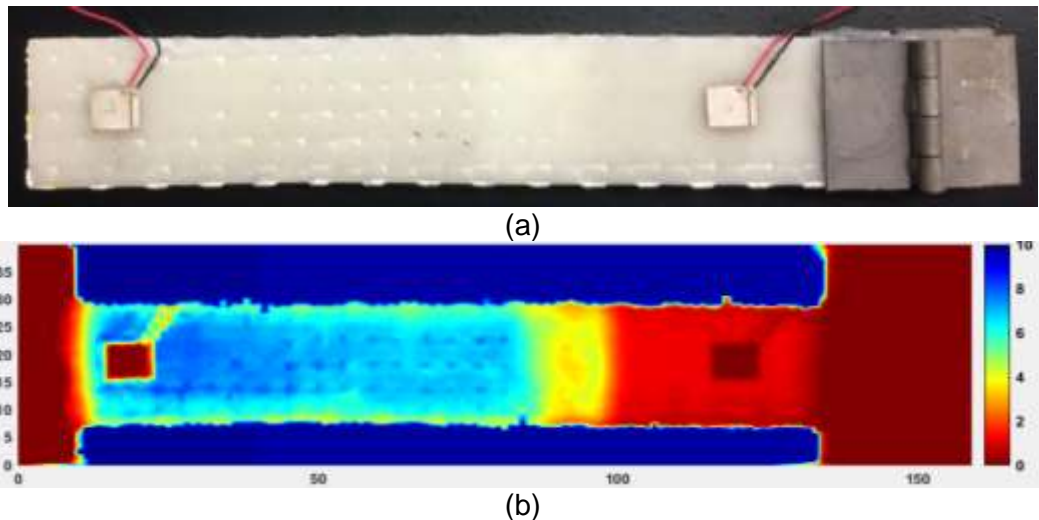


Figure 2. (a) GFRP sample with delamination induced by Mode 1 testing (b) OTS image.

### **Delamination detection using Guided Waves(GW)**

Delamination detection using GW technique involves four sequential steps. In Step 1, the appropriate excitation frequency is identified. Dispersion curves for selected material is initially obtained and excitation frequency is chosen to avoid complex wave modes. Typically, the  $A_0$  and  $S_0$  mode is excited. Step 2 involves selecting specific piezoelectric transducers and

attaching them to the specimen. PZT's with resonate frequency close to excitation frequency are attached at both the ends of the specimen (see Fig 2.a). The distance between the transducers and initial delamination is carefully measured. It is important to fix the receiver PZT at least 2.5 cm from the edge of the sample in order to avoid signals from reflection at the edges. In Step 3, a MATLAB script is developed to control the waveform generator and excite the transducer and also record the signal form the other transducer via an oscilloscope. The received signal depends on the material properties, specimen geometry and distance between the transducers. Step 4 is to analyze the time of flight (TOF) from the received GW signal. The TOF change is attributed to the increased traveling distance induced by the damage for the wave from the transducer to receiver sensor. The above steps are repeated at periodic intervals after each round the sample is subjected to fatigue loading cycles.

### **Prognosis by Particle Filtering**

In recent years, Bayesian inference has been widely implemented for fault diagnostics and prognostics applications [14,15]. Using this approach, observed data can be incorporated to estimate underlying model parameters, which can predict future health status by considering the likelihood of past and current measurements. Bayesian inference adheres to the following Bayes theorem.

$$P(\theta|z) = L(z|\theta)P(\theta)$$

where  $\theta$  is vector of unknown parameters,  $z$  is the set of known measurements,  $L(z|\theta)$  is the likelihood or the PDF of  $z$  conditional on parameters  $\theta$ ,  $P(\theta)$  is the prior PDF of  $\theta$ , and  $P(\theta|z) =$  is the posterior PDF of  $\theta$  conditional on  $z$ .

Particle filtering (PF) based on Bayes inference has lately gained popularity in structural health monitoring and prognosis owing to their consistent theoretical foundation to handle model non-linearities and non-Gaussian observation noise during estimation of model parameters [16,17]. In this approach, the conditional probability is approximated by a 'swarm' of points, known as 'particles'. These particles constitute discrete samples with weights associated with them representing their probability masses. Particles can be generated and recursively updated given the measurement model ( $h$ ), a set of available measurements  $Z = \{z_k, k \in N\}$  and an initial PDF of parameters. Using this idea Orchard and Vachtsevanos presented a failure prognostic model to predict the evolution in time of the fault indicator and compute the PDF of RUL of the faulty subsystem. The mathematical theory underlying PF algorithm is described in detail in [16].

A simple form of the empirical degradation model is described by an exponential function in equation (1) where  $a$ ,  $b$  are model parameters,  $t$  is the time or no. of cycles, and  $x$  is the damage state of the sample such as crack length, delamination area, stiffness reduction etc.

$$x = ae^{-bt} \quad (1)$$

It is important to note that inspection by NDE methods is often affected by noise and therefore noise should be taken into account when NDE measurements are used for prediction of future damage state of a structure. Hence, the measurement model is defined as:

$$z_k = h(x_k, \omega_k) \quad (2)$$

where,  $\omega_k$  is the measurement noise which can be assumed to be white Gaussian noise with variance  $\sigma$ . According to degradation model in equation (1), if  $t_k = t_{k-1} + \Delta t$ , the damage state is updated as:

$$x_k = ae^{(-b_k \Delta t)} x_{k-1} \quad (3)$$

If 'a' is considered to be a known fixed value and  $k$  is the time step index or index of loading cycle at which sample is scanned, the unknown parameters to be estimated is  $\theta = \{x, b, \sigma\}$ , including the damage state  $x_k$  which is obtained based on the model parameters  $b_k$ .

Assuming  $\omega_k$  is normally distributed, the likelihood of the measurement is defined as:

$$L(z_k | x_k^i, b_k^i, \sigma_k^i) = \frac{1}{\sqrt{2\pi\sigma_k^i}} \exp \left[ -\frac{1}{2} \left( \frac{z_k - x_k^i(b_k^i)}{\sigma_k^i} \right)^2 \right] \quad (4)$$

Under PF framework, Bayes updating is achieved by duplicating particles with higher likelihood of generating measurements  $z_k$  and discarding particles with lower likelihood to generate the new posterior PDF. This is repeated for 'k' iterations at the end of which the model parameters are estimated and used to predict future damage state of the structure.

## Experimental Setup and Results

### Material

GFRP composite samples, used in our experiment, were manufactured using a vacuum assisted liquid molding process. The reinforcement was S2-glass plain weave fabric with areal weight of 818 g/m<sup>2</sup>, namely Shield-Strand® S, provided by Owens Corning. The GFRP samples comprised six layers of such fabrics stacked at the same angle. The distribution medium was Resinflow 60 LDPE/HDPE blend fabric from Airtech Advanced Materials Group. The resin was SC-15, a two part toughened epoxy obtained from Applied Poleramic. The GFRP plate (150×300 mm) was manufactured in a 609.6 ×914.4 mm aluminum mold with point injection and point venting. Two teflon sheets of dimensions 50×150 mm with density 2.16g/cm<sup>3</sup> and tensile strength of 3900psi were inserted in between third and fourth layer of GFRP fabrics at the two edges of the plate. After the materials were placed, the mold was sealed using a vacuum bag and sealant tape, and it was then infused under vacuum at 29 in Hg. The resin-infused panel was cured in a convection oven at 60°C for two hours and post-cured at 94°C for four hours. Finally, mode 1 samples with dimensions of 150 ×25× 2 mm were cut from the manufactured GFRP plate using a diamond saw. Figure 3 shows a mode 1 sample used in our experiments which is made of 6 layers with a teflon sheet of length 50mm inserted from the edge in between third and fourth layer of the plate. The design of the sample adheres to ASTM D7791 - 17 standard for mode 1 samples intended for fatigue testing. 'As the teflon inserts are ultra-thin, they have no mechanical contribution to the sample but are used solely to create initial delamination in the specimen. Each mode-1 specimen is characterized with Young's modulus of 26 GPA, density 1907 Kg/cm<sup>3</sup> and the poisson's ratio of 0.17 (material is assumed to be quasi-isotropic).

### MTS setup for fatigue testing

The above GFRP specimen is subjected to tension-tension fatigue testing under 810 Material Test System (MTS) machine with 50kN load cell. At first, the critical displacement where the specimen cracks is recorded by introducing monotonic loading to five similar samples. The process is repeated for all the specimens and the average critical displacement is computed. Fatigue loading is then conducted on a new sample under cyclic loading at 5 cycles/sec and displacement ratio of 0.1. The experimental setup for Mode 1 GFRP sample subjected to cyclic loading in MTS machine is illustrated in Figure 3.

### OTS results

OTS images of a mode 1 GFRP sample subjected to 9 rounds of cyclic loading is presented

in Figure 4. An iBeam-smart-640s laser diode with 640 nm fundamental wavelength, ~1.5 mm beam diameter and 3.1 mW output power was used as the light source. The OTS system was placed on an active vibration isolation table and optical scans were acquired in dark ambience with a 1 mm step size.

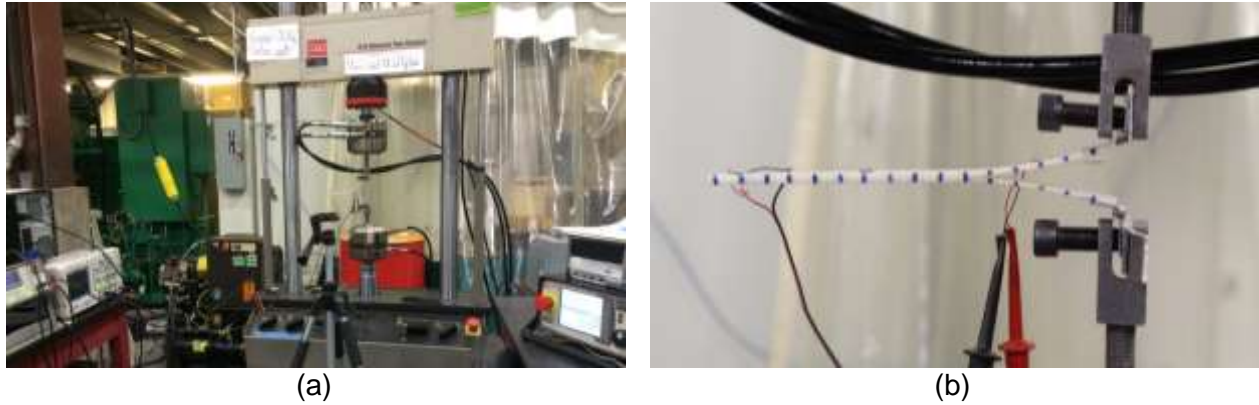


Figure 3. (a) Experimental setup for Mode 1 GFRP sample subjected to cyclic loading in MTS machine, (b) Enlarged image of GFRP sample under Mode 1 test.

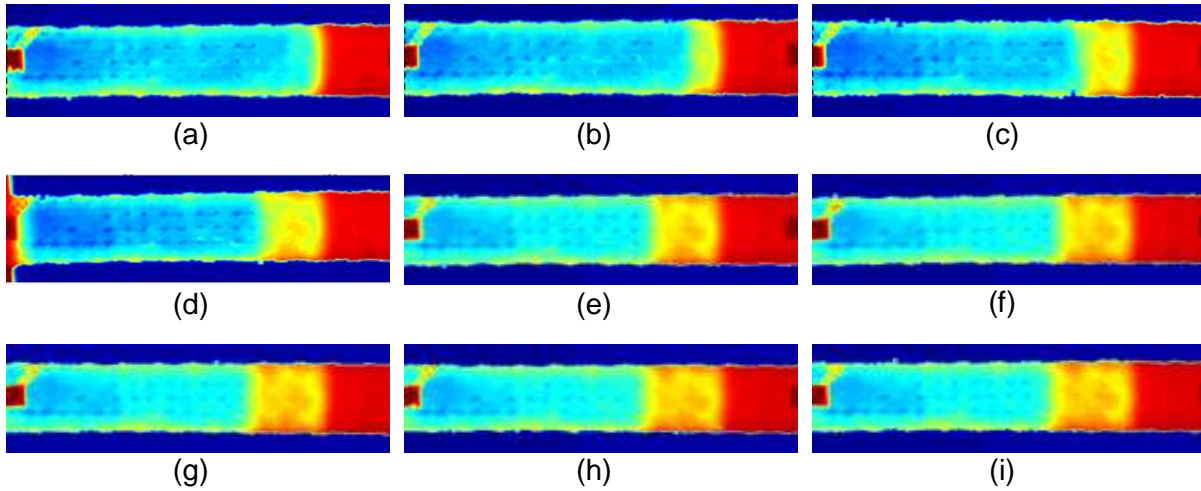


Figure 4. OTS images of a GFRP sample (a) Healthy sample and on being subjected to Mode 1 cyclic loading after (b) 20K cycles (c) 40K cycles (d) 60K cycles (e) 80K cycles (f) 100K cycles (g) 120K cycles (h) 140K cycles (i) 160 cycles.

From the OTS images, extent of delamination can be observed as the region between end of teflon and the beginning of healthy part of the sample. As expected, delamination grows inside the sample with increase in number of load cycles. Area of delamination from the scanned image is computed using image processing algorithm implemented in MATLAB, as depicted in Figure 5. The delaminated area is identified using segmentation via fast marching method [18] to generate the gray scale image shown in Figure 5.c. The total number of pixels that are 'turned on' provides the area of delamination in terms of pixels ( $d_{pix}$ ).

The piezoelectric sensors attached to the GFRP sample mark as reference points and are used to calculate the physical area of delamination from  $d_{pix}$ . Using cluster-based-segmentation followed by connected components [19], location of the two pzt sensors are identified and the pixel distance between their inner edges is recorded as  $l_{pix}$ . Additionally, edge detection algorithm is implemented to determine the upper and lower edges of the sample



and its pixel width is recorded as  $w_{pix}$ . Measuring the physical distance between two PZT sensors ( $L_{phy}$ ) and width of the sample ( $W_{phy}$ ), the delamination area ( $D_{phy}$ ) is calculated according to equation (5). In this paper,  $L_{phy} = 10\text{ cm}$  and  $W_{phy} = 2.5\text{ cm}$ .

$$D_{phy} = \left( \frac{d_{pix}}{l_{pix} \times w_{pix}} \right) (L_{phy} \times W_{phy}) \text{ cm}^2 \quad (5)$$

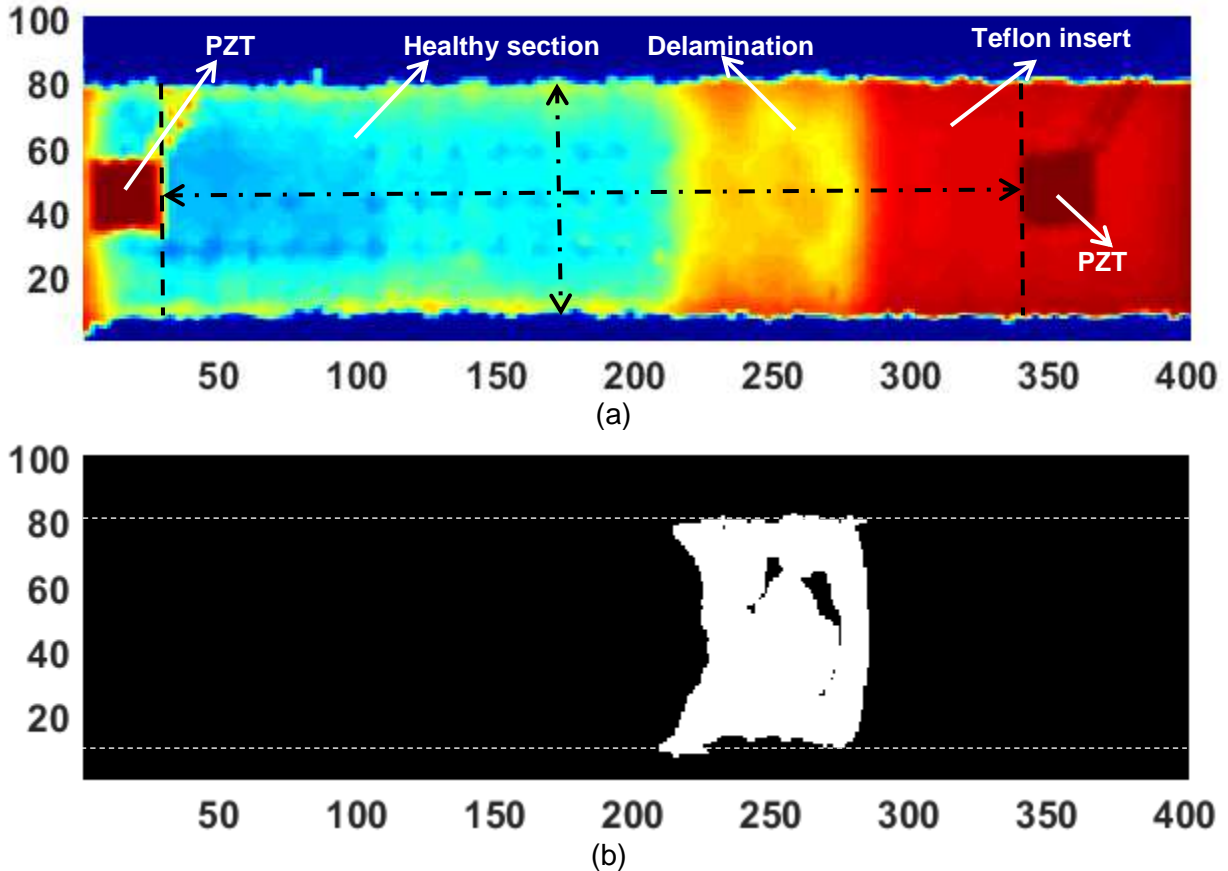


Figure 5. (a) Fatigues GFRP sample after 160K load cycles (b) OTS image of delaminated sample (c) Binary image denoting delamination area identified after image processing.

Area of delamination is computed for each of the OTS images depicted in Figure 4, after every interval 20K load cycles. Plot of delamination area against number of load cycles is shown in Figure 6.

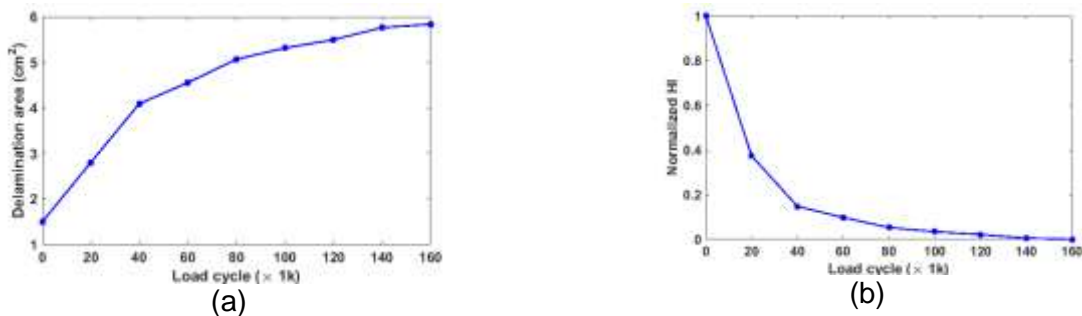


Figure 6. Plot of number of load cycles versus (a) delamination area (from OTS measurements) and (b) Normalized Health Index (HI).

The first step for prognosis is to define a health index (HI) that indicates the current health status of the sample subjected to damage. In this paper HI for  $i^{th}$  round of fatigue experiment is defined as:

$$HI(i) = x(i) = \frac{1}{D_{phy}(i)} \text{ cm}^{-2} \quad (6)$$

$$\text{After normalizing, } HI(i) = \frac{x(i) - \min(x(i))}{\max(x(i)) - \min(x(i))} \quad (7)$$

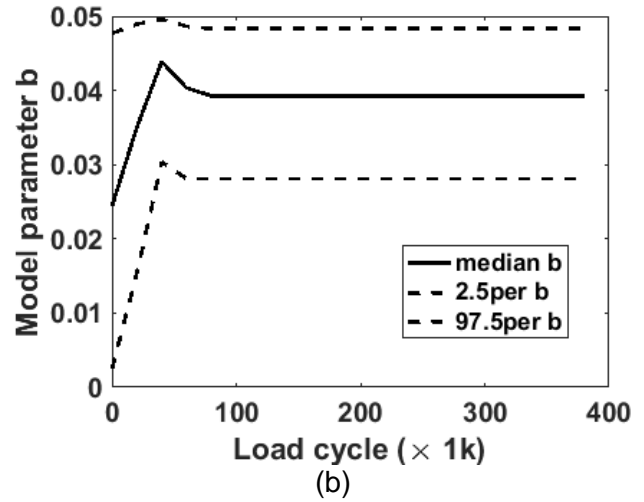
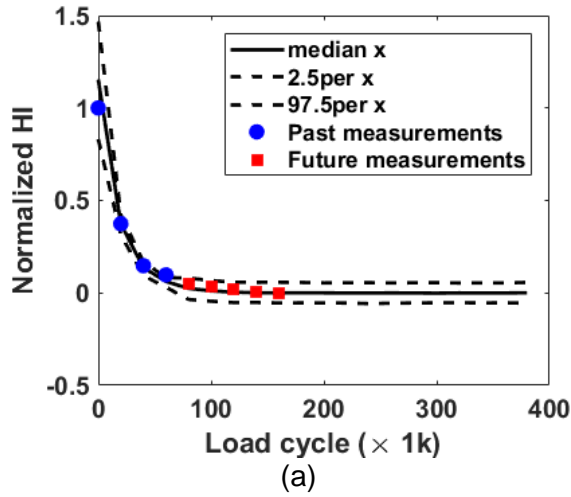
The primary objective of prognosis is to predict future HI by utilizing known HI values derived from past measurements. In order to validate the proposed prognosis approach, the first five measurements (from a total of 9 HI values) are considered to develop the damage growth model and estimate future four measurements. The difference between HI calculated from true measurements and their estimated values assess the performance of the prognosis algorithm.

Based on the behavior of HI from Figure 6.b, an exponential model described in equation (1) is implemented as damage propagation model for describing delamination growth in the mode 1 composite sample due to fatigue. Here  $a = 1$ . Starting with uniform initial distributions for all the parameters (equation (8)), the likelihood of 5000 particles are computed according to equation (4). Finally, the posterior distribution of particles is computed for five iterations to update the model parameter ' $b$ ' using the five known HI data. The estimated HI curve is denoted in Figure 7 along with 95 percentile confidence bounds.

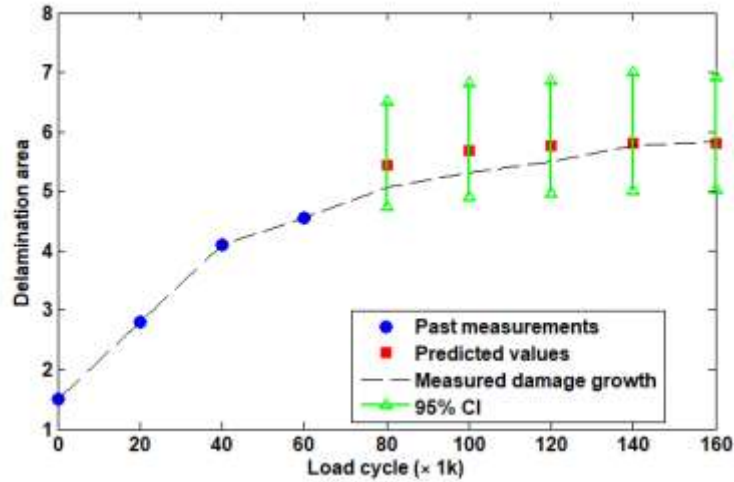
$$x \sim \text{Uniform}(0.5, 1.5) \quad (8)$$

$$b \sim \text{Uniform}(0, 1)$$

$$\sigma \sim \text{Uniform}(0.01, 0.05)$$







(c)

Figure 7. (a) Predicted exponential model using past measurements with 95 percentile confidence bounds (b) Updating path of model parameter 'b' (c) Predicted delamination area using past measurements.

No. of Load cycles	Measured delamination area	Predicted delamination area	95% Confidence Interval
80	5.0683	5.4604	[4.77,6.52]
100	5.3156	5.6743	[4.91,6.75]
120	5.4968	5.7653	[4.95,6.88]
140	5.7629	5.7918	[ 5.01,6.89]
160	5.8376	5.8289	[5.03,6.92]

Table 1. Measured and predicted delamination areas from prognosis algorithm using exponential model on OTS data.

### GW results

Guided wave experimental setup consists of the MTS, oscilloscope, function generator and a computer. With the available mechanical properties of GFRP specimen, dispersion curves are generated. From the dispersion curves, excitation frequency of 40 KHz is chosen to avoid higher order modes. A Gaussian pulse of 40 kHz with peak voltage of 10 volts is generated using the function generator which excites the transducer PZT. The generated lamb waves are then sensed by the receiver PZT attached on the Teflon section. Figure 8.a and 8.b shows the schematic of the experimental setup and the corresponding excited and received signals. Owing to the small the distance between the two transducers, anti-symmetric and symmetric modes are mixed as seen in the Figure 8.b. Also, reflections from the edges of the specimen make the received signal complex. However, the TOF between the received and transmitted signal can be clearly identified.

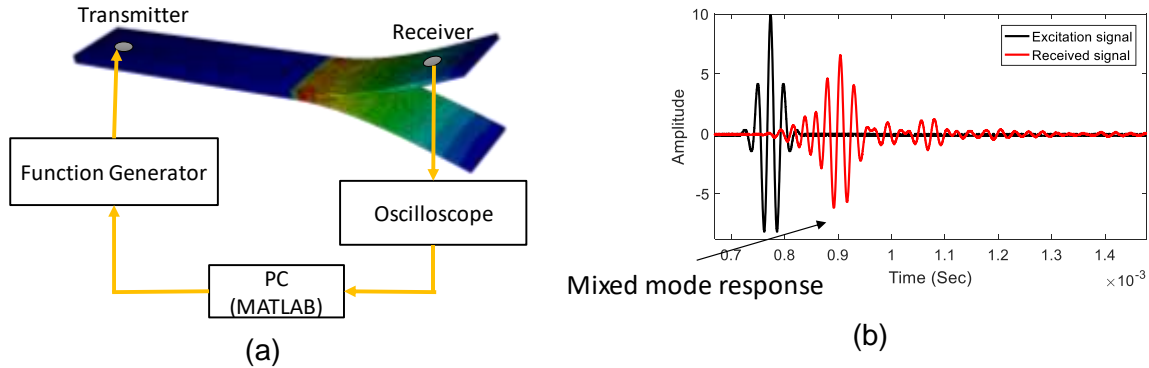


Figure 8. (a) Schematic of GW experimental setup (b) Excited and received signals in healthy sample.

The same 6-layered GFRP sample is monitored using GW setup in addition to OTS, after every 20K fatigue cycles. Due to increase in delamination area, the time of flight between received and transmitted signal increases. The increment in TOF, also referred to as the change on phase of received GW signal is computed for 8 rounds of tension-tension loading of the sample. Figure 9.a shows the phase shift between the healthy sample and sample after 160K load cycles. Figure 9.b illustrates the normalized phase change form healthy to 160K fatigue cycles at an interval of 20K cycles. A steady growth in phase change is noticed which can be correlated to the increase in delamination area inside the specimen.

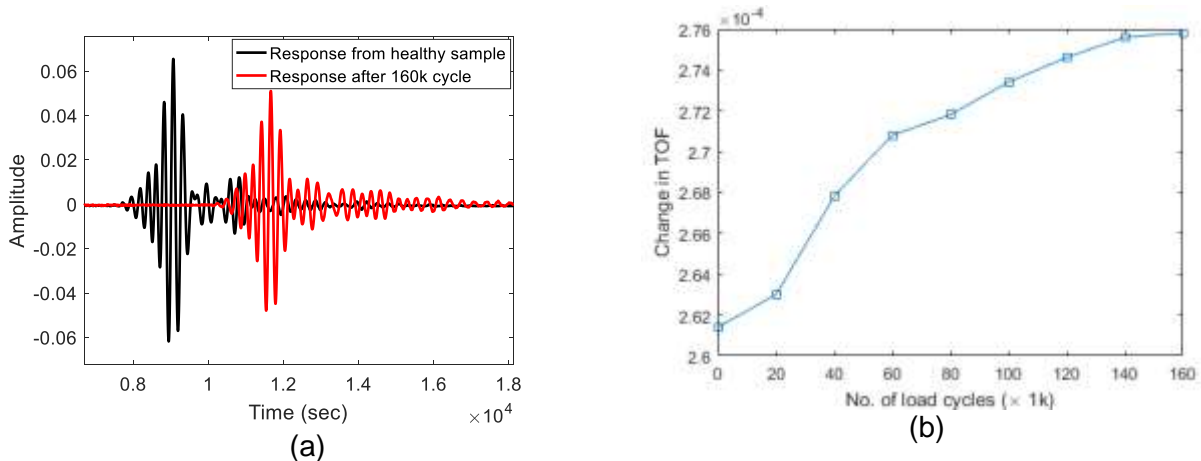


Figure 9. (a) Received signal between healthy sample and sample after 160K cycle (b) change Trend of change in TOF between received and excited signal with increase in number of fatigue cycles.

Similar to OTS data, the normalized health index for GW dataset is computed according to equation (6) and (7), where  $x(i)$  is the TOF change obtained at end of every 20K load cycles. The same exponential model is implemented as the damage propagation model and parameter 'b' is estimated using particle filtering approach using first four GW measurements. Values for fixed parameter and initial distribution of unknown parameters are kept unchanged as stated in equation (8).

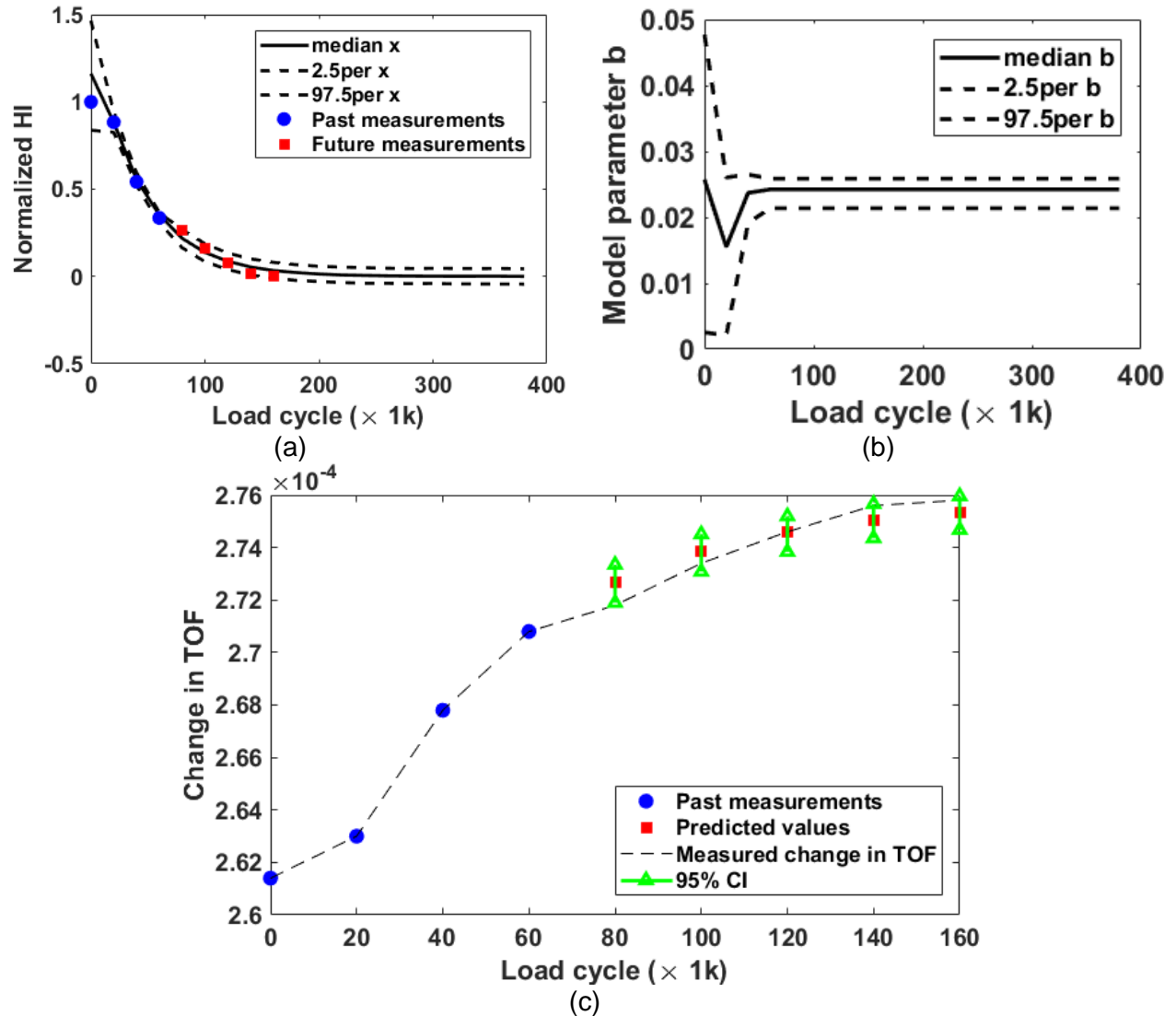


Figure 10. (a) Predicted exponential model using past measurements with 95 percentile confidence bounds (b) Updating path of model parameter 'b' (c) Predicted change in TOF using past measurements.

No. of Load cycles	Measured change in TOF ( $\times 10^{-4}$ )	Predicted change in TOF ( $\times 10^{-4}$ )	95% Confidence Interval ( $\times 10^{-4}$ )
80	2.718	2.726	[2.719, 2.733]
100	2.734	2.738	[2.730, 2.745]
120	2.746	2.746	[2.738, 2.751]
140	2.756	2.750	[2.743, 2.756]
160	2.758	2.753	[2.746, 2.759]

Table 2. Measured and predicted change in TOF value from prognosis algorithm using exponential model on GW data.

## Conclusion and Future Work

This paper presents an application of two NDE methods for prediction of fatigue induced delamination area in GFRP samples introduced by tension-tension fatigue tests. OTS and GW successfully detect growth of delamination in the composite laminate. Both the sensors are well suited for practical usage in industries to inspect composite materials. Owing to high detection capability of OTS system, it can be used as a benchmark to validate PZT sensors. Additionally, OTS system can be implemented for detecting defects in painted or coated GFRP materials as long as a laser source of suitable wavelength is used. However, OTS is inherently restricted to glass-fibers and epoxy resins which have good transmission properties and cannot be used for diagnosis of carbon-fibers. By defining a health index based on area of delamination, a simple exponential model could be defined to describe the fatigue damage progression. Results from implementing particle filtering technique are promising as future damage areas could be predicted accurately within confidence bounds.

This is an on-going study with initial results presented in this paper. Future work should include more fatigue experiments until the GFRP sample reaches the failure threshold where the joint structure cannot sustain any further load.. Knowing the end-of-life criterion, remaining-useful-life (RUL) of the sample should be computed. This paper presents an empirical model for damage propagation. In future, fatigue induced delamination should be investigated in depth and additional parameters affecting internal damage growth should be considered for developing a more robust physics-based model. Moreover, other NDE techniques should also be used to diagnose current and predict future health of composite structures. Novel ways to improve prediction of RUL in composite samples through data-fusion of multiple NDE measurements is another interesting research area to be explored.

## References

1. Zou, Y., Tong, L. P. S. G., & Steven, G. P. (2000). Vibration-based model-dependent damage (delamination) identification and health monitoring for composite structures—a review. *Journal of Sound and vibration*, 230(2), 357-378.
2. McCombe, G. P., Rouse, J., Trask, R. S., Withers, P. J., & Bond, I. P. (2012). X-ray damage characterisation in self-healing fibre reinforced polymers. *Composites Part A: Applied Science and Manufacturing*, 43(4), 613-620.
3. De Oliveira, R., & Marques, A. T. (2008). Health monitoring of FRP using acoustic emission and artificial neural networks. *Computers & structures*, 86(3), 367-373.
4. Akuthota, B., Hughes, D., Zoughi, R., Myers, J., & Nanni, A. (2004). Near-field microwave detection of disbond in carbon fiber reinforced polymer composites used for strengthening cement-based structures and disbond repair verification. *Journal of materials in civil engineering*, 16(6), 540-546.
5. Harris, B. (Ed.). (2003). *Fatigue in composites: science and technology of the fatigue response of fibre-reinforced plastics*. Woodhead Publishing.
6. Miyano, Y., Nakada, M., & Sekine, N. (2005). Accelerated testing for long-term durability of FRP laminates for marine use. *Journal of composite materials*, 39(1), 5-20.
7. Corbetta, M., Sbarufatti, C., Saxena, A., Giglio, M., & Goebel, K. (2016). Model-based fatigue prognosis of fiber-reinforced laminates exhibiting concurrent damage mechanisms.
8. Khomenko, A., Karpenko, O., Koricho, E., Haq, M., Cloud, G. L., & Udpa, L. (2016). Theory and validation of optical transmission scanning for quantitative NDE of impact damage in GFRP composites. *Composites Part B: Engineering*, 107, 182-191.
9. Dong Wang, Lin Ye, Youhong Tang, & Ye Lu (2012). "Monitoring of delamination onset and growth during Mode I and Mode II interlaminar fracture tests using guided waves". *Composites Science and*

10. Chiachio, J., Chiachio, M., Saxena, A., Rus, G., & Goebel, K. (2014). A model-based prognostics framework to predict fatigue damage evolution and reliability in composites. *Prognostics and Health Management Society, Nantes, France2014. EPHM*, 732-742.
11. Peng, T., Saxena, A., Goebel, K., Sankararaman, S., Xiang, Y., & Liu, Y. (2013). Probabilistic delamination diagnosis of composite materials using a novel Bayesian Imaging Method. In *2013 Annual Conference of the Prognostics and Health Management Society, PHM 2013*. Prognostics and Health Management Society.
12. Peng, T., Liu, Y., Saxena, A., & Goebel, K. (2015). In-situ fatigue life prognosis for composite laminates based on stiffness degradation. *Composite Structures*, 132, 155-165.
13. Khomenko, A., Karpenko, O., Koricho, E., Haq, M., Cloud, G., & Udpa, L. (2016, April). Optical transmission scanning for damage quantification in impacted GFRP composites. In *SPIE Smart Structures and Materials+ Nondestructive Evaluation and Health Monitoring* (pp. 98040R-98040R). International Society for Optics and Photonics.
14. Zhao, F., Tian, Z., & Zeng, Y. (2013). Uncertainty quantification in gear remaining useful life prediction through an integrated prognostics method. *IEEE Transactions on Reliability*, 62(1), 146-159.
15. Beck, J. L., & Au, S. K. (2002). Bayesian updating of structural models and reliability using Markov chain Monte Carlo simulation. *Journal of engineering mechanics*, 128(4), 380-391.
16. Orchard, M. E., & Vachtsevanos, G. J. (2009). A particle-filtering approach for on-line fault diagnosis and failure prognosis. *Transactions of the Institute of Measurement and Control*, 31(3-4), 221-246.
17. Zio, E., & Peloni, G. (2011). Particle filtering prognostic estimation of the remaining useful life of nonlinear components. *Reliability Engineering & System Safety*, 96(3), 403-409.
18. Koschan, A. F. (2003, June). Perception-based 3D triangle mesh segmentation using fast marching watersheds. In *Computer Vision and Pattern Recognition, 2003. Proceedings. 2003 IEEE Computer Society Conference on* (Vol. 2, pp. II-II). IEEE.
19. Felzenszwalb, P. F., & Huttenlocher, D. P. (2004). Efficient graph-based image segmentation. *International journal of computer vision*, 59(2), 167-181.